

# Noninvasive Estimation of Pulsatile and Static Intracranial Pressure by Optical Coherence Tomography

Henrik Holvin Jacobsen<sup>1,2</sup>, Øystein Kalsnes Jørstad<sup>1,2</sup>, Morten C. Moe<sup>1,2</sup>, Goran Petrovski<sup>1-3</sup>, Are Hugo Pripp<sup>4</sup>, Tiril Sandell<sup>1,5</sup>, and Per Kristian Eide<sup>2,6</sup>

<sup>1</sup> Department of Ophthalmology, Oslo University Hospital-Ullevål, Oslo, Norway

<sup>2</sup> Institute of Clinical Medicine, Faculty of Medicine, University of Oslo, Oslo, Norway

<sup>3</sup> Department of Ophthalmology, University of Split School of Medicine, Split, Croatia

<sup>4</sup> Oslo Centre of Biostatistics and Epidemiology, Research Support Services, Oslo University Hospital, Oslo, Norway

<sup>5</sup> Department of Ophthalmology, Vestre Viken Hospital, Drammen, Norway

<sup>6</sup> Department of Neurosurgery, Oslo University Hospital-Rikshospitalet, Oslo, Norway

**Correspondence:** Per Kristian Eide, Department of Neurosurgery, Oslo University Hospital-Rikshospitalet, Pb 4950 Nydalen, N-0424 Oslo, Norway.

e-mail: [p.k.eide@medisin.uio.no](mailto:p.k.eide@medisin.uio.no)

**Received:** August 21, 2021

**Accepted:** December 17, 2021

**Published:** January 20, 2022

**Keywords:** optical coherence tomography; intracranial pressure; pulsatile pressure; noninvasive

**Citation:** Jacobsen HH, Jørstad ØK, Moe MC, Petrovski G, Pripp AH, Sandell T, Eide PK. Noninvasive estimation of pulsatile and static intracranial pressure by optical coherence tomography. *Transl Vis Sci Technol.* 2022;11(1):31, <https://doi.org/10.1167/tvst.11.1.31>

**Purpose:** To explore the ability of optical coherence tomography (OCT) to noninvasively estimate pulsatile and static intracranial pressure (ICP).

**Methods:** An OCT examination was performed in patients who underwent continuous overnight monitoring of the pulsatile and static ICP for diagnostic purpose. We included two patient groups, patients with idiopathic intracranial hypertension (IIH;  $n = 20$ ) and patients with no verified cerebrospinal fluid disturbances (reference;  $n = 12$ ). Several OCT parameters were acquired using spectral-domain OCT (RS-3000 Advance; NIDEK, Singapore). The ICP measurements were obtained using a parenchymal sensor (Codman ICP MicroSensor; Johnson & Johnson, Raynham, MA, USA). The pulsatile ICP was determined as the mean ICP wave amplitude (MWA), and the static ICP was determined as the mean ICP.

**Results:** The peripapillary Bruch's membrane angle (pBA) and the optic nerve head height (ONHH) differed between the IIH and reference groups and correlated with both MWA and mean ICP. Both OCT parameters predicted elevated MWA. Area under the curve and cutoffs were 0.82 (95% confidence interval [CI], 0.66–0.98) and  $-0.65^\circ$  (sensitivity/specificity; 0.75/0.92) for pBA and 0.84 (95% CI, 0.70–0.99) and 405  $\mu\text{m}$  (0.88/0.67) for ONHH. Adjusting for age and body mass index resulted in nonsignificant predictive values for mean ICP, whereas the predictive value for MWA remained significant.

**Conclusions:** This study provides evidence that the OCT parameters pBA and ONHH noninvasively can predict elevated pulsatile ICP, represented by the MWA.

**Translational Relevance:** OCT shows promise as a method for noninvasive estimation of ICP.

## Introduction

Continuous monitoring of intracranial pressure (ICP) is a cornerstone in the diagnosis and management of a wide range of intracranial disorders, such as traumatic brain injury, intracranial hemorrhage, and cerebrospinal fluid (CSF) disturbances.<sup>1</sup> Still, ICP monitoring is invasive and requires insertion of a probe or catheter into the intracranial compartment, thereby carrying a risk of complications.<sup>2,3</sup> A wide range

of noninvasive methods of measuring the static and pulsatile components of ICP have been explored,<sup>1,4–11</sup> but so far, none have been found clinically suitable.

The eye is a potential window for indirect assessment of the ICP due to the direct communication between the intracranial and intraorbital subarachnoid spaces, by which the ICP directly affects the optic nerve and eye globe.<sup>12</sup> Hence, papilledema is a widely recognized indirect sign of intracranial hypertension. Recently, optical coherence tomography (OCT) has gained increasing interest as a

potential tool for noninvasive ICP assessment.<sup>13–15</sup> The OCT methodology measures the reflection of back-scattered light and allows for detection and quantification of even subtle morphologic changes in the retina and the optic nerve.<sup>16</sup> In patients with idiopathic intracranial hypertension (IIH),<sup>17</sup> the static ICP (mean ICP), measured using a telemetric parenchymal ICP probe, correlated with OCT measures of the optic nerve head. Moreover, in a pediatric study,<sup>18</sup> OCT measurements of the retina and the optic nerve head detected elevated mean ICP, measured with a subdural probe. However, with the exception of these studies, the published reports on estimating ICP from OCT have merely studied the relationship between OCT findings and the lumbar CSF opening pressure.<sup>13–15,19–22</sup> The CSF opening pressure (usually measured in mm H<sub>2</sub>O) provides an indirect estimate of the ICP (usually measured in mm Hg) and has been shown to differ from the ICP measured dynamically with an intracranial probe.<sup>1,23</sup> Furthermore, the CSF opening pressure only provides a snapshot of the ICP and may be misleading due to fluctuations of ICP over time.<sup>24</sup>

Previous studies have only examined the static ICP, even though ICP consists of both static and pulsatile ICP. The latter results from the pressure fluctuations created by the cardiac contractions.<sup>1</sup> The pulsatile ICP may be expressed as the mean wave amplitude (MWA)<sup>25</sup> and has been reported to better reflect the pressure-volume reserve capacity (or intracranial compliance) than the static ICP.<sup>1,26</sup>

This study explored the ability of OCT to noninvasively estimate the MWA and the mean ICP that were measured overnight as part of a diagnostic workup.

## Methods

### Approvals

The ICP scores are stored as part of a Neurovascular-Cerebrospinal fluid quality registry approved by the Institutional Review Board of Oslo University Hospital (2011/6692). The OCT assessment was done as part of a study approved by the Regional Committee for Medical and Health Research Ethics of Health Region South-East, Norway (2018/1074). The study was conducted according to the ethical standards of the Declaration of Helsinki from 1975 and as revised in 1983. Informed consent was given by the participants prior to inclusion.

### Design

A prospective observational study design was used. In order to examine how OCT parameters could estimate pulsatile and static ICP scores, we (1) compared OCT and ICP scores between two patient groups, (2) correlated the OCT with the ICP scores of individual patients, and (3) determined the predictive ability of OCT on ICP.

### Patients

#### IIH Group

The first group included patients who fulfilled the diagnostic criteria for IIH.<sup>27</sup> The patients had initially been diagnosed and treated locally but referred to the Department of Neurosurgery because of failed conservative medical treatment. ICP monitoring was performed in the workup for shunt surgery.

#### Reference Group

The second group included age-matched patients who had undergone ICP monitoring in the workup for suspected CSF disturbances. In these patients, no apparent CSF disturbances could be verified through imaging studies, and accordingly, surgical intervention was not performed. However, because all patients in the second group had symptoms, they cannot be regarded as healthy.

### Overnight ICP Monitoring

Both groups underwent overnight ICP monitoring at the Department of Neurosurgery, Oslo University Hospital–Rikshospitalet, Norway. Monitoring of the ICP was performed overnight as part of routine clinical workup in order to diagnose and select patients for CSF diversion surgery.<sup>28</sup> Continuous ICP waveforms were recorded at 100 to 200 Hz using an intracranial pressure sensor (Codman ICP MicroSensor; Codman, Johnson & Johnson, Raynham, MA, USA) placed 1 to 2 cm into the parenchyma through a burr hole in the frontal bone under local anesthetics.<sup>25</sup> For the MWA, single heartbeat-induced pressure waves were identified by an automatic algorithm, and the pulse amplitude was calculated as the pressure difference between the diastolic and systolic pressures over 6-second time windows.<sup>25</sup> The mean ICP is the sum of all pressure measurements during the 6-second time windows divided by the number of measurements. With regard to our previously reported upper normal ICP scores,<sup>28,29</sup> abnormal pulsatile ICP was defined by average overnight MWA scores  $\geq 4$  mm Hg and/or  $\geq 5$  mm Hg in  $\geq 10\%$  of the recording time, and

abnormal static ICP was defined by overnight average mean ICP  $\geq 15$  mm Hg and/or  $\geq 10\%$  of measurements  $\geq 15$  mm Hg.

## Ophthalmologic Examination and OCT Imaging Protocol

All ophthalmic examinations were performed at the Department of Ophthalmology, Oslo University Hospital–Ullevål, Norway, by an experienced ophthalmic nurse and one author (HHJ). To avoid dependent data, only the “worst eye” defined by mean defect on threshold perimetry was included. Exclusion criteria were refraction error with spherical equivalent outside the range of  $-6.0$  to  $+3.0$  diopters, concurrent eye disorders affecting the retina or optic nerve, and OCT scans with artifacts or poor quality (signal strength index  $<7$  of 10).

Standard white-on-white threshold perimetry of the central  $30^\circ$  was performed using an Octopus 900 perimeter (Haag-Streit AG, Koeniz, Switzerland) and the G-TOP program. The perimetry was performed by a trained ophthalmic nurse. Presence of fundoscopic papilledema was evaluated by one author (HHJ) and graded as present or not present.

Spectral-domain OCT scans were acquired in mydriasis using a RS-3000 OCT Advance (NIDEK, Singapore) and its Navis-EX software (NIDEK).

The peripapillary Bruch’s membrane angle (pBA) (Fig. 1) and the maximum optic nerve head height (ONHH) (Fig. 2) were measured manually on 6-mm horizontal B-scans traversing through the center of the optic disc. For both measurements, consensus was reached between two observers. Measurements of the pBA were performed in Adobe Photoshop (Adobe, San Jose, CA, USA). The peripheral sections of the nasal and temporal Bruch’s membrane were used as reference. Reference lines were obtained by drawing lines parallel to the Bruch’s membrane in the nasal and

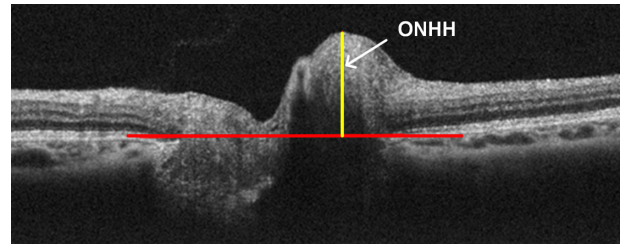


**Figure 2.** The ONHH. A line connecting both sides (nasal-temporal) of the scleral canal opening (*red line*) was used as a reference line. The height was measured from the highest point of the optic nerve head to the reference line (*yellow line*).

temporal periphery of the scan. The angle for which the central section of Bruch’s membrane deviated from the reference lines was determined nasally and temporally; the mean of the two angles constitutes the pBA. The angle was denoted negative if deviating posteriorly (i.e., away from the vitreous) and positive if deviating anteriorly. For the ONHH measurement, we used the Navis-EX software. A reference line was drawn across the scleral opening, connecting the nasal and temporal ends of the retinal pigment epithelium/Bruch’s membrane layers. The ONHH was measured by a straight line to the highest point of the optic nerve head (Fig. 2). The OCT parameters mean retinal nerve fiber layer (RNFL), mean peripapillary total retinal thickness (TRT), and macular ganglion cell complex (mGCC) were also measured and compared between the groups. The mean RNFL thickness and the mean TRT were automatically measured by the Navis-EX software using a ring scan centered at the optic disc with a diameter of 3.45 mm. The mean TRT was measured from the inner limiting membrane to the retinal pigment epithelium/Bruch’s membrane. The mean mGCC was measured automatically by the Navis-Ex software using the 9-mm  $\times$  9-mm Macular Map program.

## Statistical Analyses

An independent *t*-test and a Pearson  $\chi^2$  test were used for the comparison of continuous data between the groups. Correlations between independent variables were determined by the Pearson correlation coefficient. Logistic regression models calculated the odds ratio for continuous exposure variables. The optimal cutoff point for a diagnostic test was calculated from the receiver operating curves (ROCs) using the Liu method. SPSS version 27 (IBM Corporation, Armonk, NY, USA) or Stata/SE version 15.0 (StataCorp LLC, College Station, TX, USA) with the user-developed command *cutpt*<sup>30</sup> was used for the

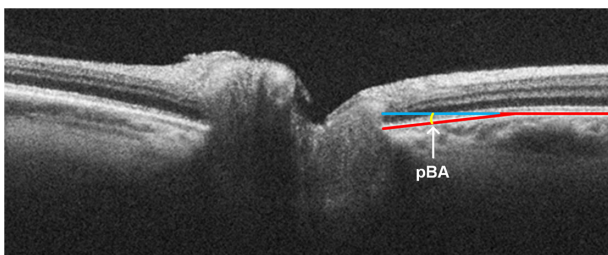


**Figure 1.** The pBA. The Bruch’s membrane/retinal pigment epithelium is marked by a *red line*. The pBA (*yellow*) is the angle that is formed between the deviated peripapillary Bruch’s membrane (*red line*) and the unaltered part (*blue line*). A mean of nasal and temporal angles was calculated.

statistical calculations. Accepted statistical significance was  $\leq 0.05$ .

## Data Availability

The data by which this article is based are available upon reasonable request.

## Results

### Patients

The study groups consisted of 20 patients fulfilling the diagnostic criteria of IIH<sup>27</sup> and 12 reference (REF) patients (Table 1). Patients were included during the study period from September 2018 to November 2020. The patient groups were comparable with regard to age, spherical equivalent, and body mass index (BMI) (Table 1). However, the IIH group had a higher proportion of females than the REF group.

The clinical indications for the ICP monitoring in the REF group were the following: symptoms and complaints that were tentatively associated with imaging findings of a pineal gland cyst ( $n = 7$ ), clini-

cal suspicion of spontaneous intracranial hypotension ( $n = 1$ ), and initial suspicion of IIH that was later ruled out ( $n = 4$ ). Since diagnostic workup, including imaging and ICP measurements, in these patients failed to identify any abnormalities, it was concluded that they did not have apparent CSF disturbance.

There were 12 patients using ICP-lowering medications (acetazolamide,  $n = 11$ ; topiramate + furosemide,  $n = 1$ ) at the ophthalmic examination; 10 of 12 received the same therapy at the time of ICP measurement. One patient discontinued medications but had a spinal tap performed prior to the ICP measurement, and one patient had a dose increase (acetazolamide 1.5 g at the ophthalmic examination to 2.25 g at the ICP measurement).

### Comparison of ICP and OCT Parameters Between the Groups

The IIH group had significantly higher overnight pulsatile ICP (MWA) and static ICP (mean ICP) than the REF group. The intraocular pressure did not differ between the groups (Table 1). According to our previously described upper normal threshold values for MWA and mean ICP,<sup>28,29</sup> the MWA was abnormal in

**Table 1.** Information About Demographics and ICP and OCT Scores

Characteristic	IIH	REF	P Value
Number	20	12	
Gender (female/male), <i>n</i>	18/2	2/10	<0.001
Age (y)	32.3 ± 9.6	33.9 ± 8.9	ns
BMI (kg/m <sup>2</sup> )	30.4 ± 5.1	29.1 ± 4.6	ns
Papilledema (present/not present), <i>n</i>	7/13	0/12	<0.001
IOP (mm Hg)	13.2 ± 3.3	13.8 ± 3.3	ns
Spherical equivalent	-0.3 ± 1.2	-0.6 ± 0.8	ns
Overnight MWA			
Average (mm Hg)	6.7 ± 2.0	3.5 ± 0.5	<0.001
Percentage ≥5 mm Hg	70.6 ± 20.9	7.3 ± 6.7	<0.001
Overnight mean ICP			
Average (mm Hg)	13.4 ± 5.6	6.8 ± 4.9	0.003
Percentage ≥15 mm Hg	26.9 ± 28.7	8.1 ± 17.8	ns
OCT			
pBA (degrees)	-0.24 ± 3.58	-3.03 ± 2.76	0.038
ONHH (μm)	520.0 ± 139.1	385.2 ± 116.5	0.013
Mean mGCC (μm)	94.1 ± 12.7	99.2 ± 6.0	ns
Mean peripapillary RNFL (μm)	124.2 ± 77.8	101.1 ± 12.3	ns
Mean peripapillary TRT (μm)	335.7 ± 67.8	322.8 ± 11.7	ns
RNFL/mGCC	1.0 ± 0.6	1.0 ± 0.1	ns
TRT/mGCC	3.5 ± 0.5	3.3 ± 0.2	ns

Numbers given as mean ± standard deviation for continuous variables. Significant differences determined by independent samples *t*-test for continuous data and by Pearson  $\chi^2$  test for categorized data. ns, nonsignificant.

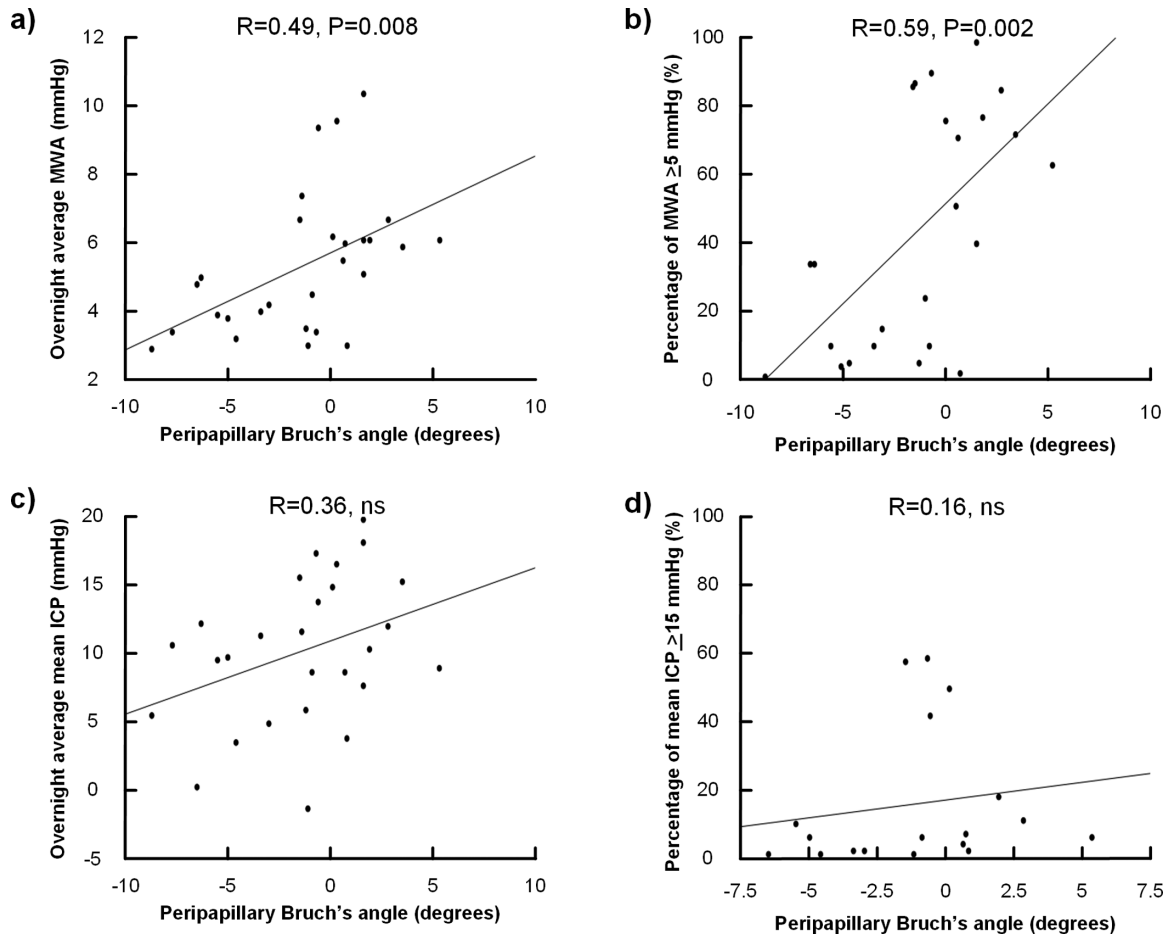


**Figure 3.** Association between the pBA and pulsatile and static ICP scores. There was a significant positive correlation between (a) the pBA and the average overnight MWA and (b) between the pBA and the overnight percentage of MWA  $\geq 5$  mm Hg. No significant correlation was found between pBA and (c) average of overnight mean ICP or (d) overnight percentage mean ICP  $\geq 15$  mm Hg. Each plot shows the fit line and Pearson correlation coefficient with significance levels. ns, nonsignificant.

19 of 20 (95%) patients in the IIH group but in none of the REF patients. The mean ICP was abnormal in 8 of 20 (40%) patients with IIH and 1 of 12 (8%) REF patients.

Regarding the OCT parameters, the pBA was significantly smaller in the IIH than the REF group, demonstrating a more anterior deflected peripapillary Bruch's membrane. The ONHH was significantly increased in the IIH group (Table 1). The other OCT parameters did not differ significantly between the groups (Table 1).

### Association Between ICP and OCT Parameters

There was a positive correlation between the OCT parameters pBA and ONHH and the ICP scores. In particular, the pBA became increasingly smaller (anteriorly deflected) with increasing pulsatile ICP,

expressed as overnight average MWA (Fig. 3a) or percentage proportion of MWA  $\geq 5$  mm Hg (Fig. 3b). This was not significant for static ICP (mean ICP; Figs. 3c, 3d). Furthermore, there was a significant positive correlation between ONHH and overnight average MWA (Fig. 4a), proportion of MWA  $\geq 5$  mm Hg (Fig. 4b), and overnight mean ICP (Fig. 4c). The proportion of mean ICP  $\geq 15$  mm Hg did not correlate with ONHH (Fig. 4d).

### Ability of OCT to Predict Abnormal Pulsatile and Static ICP

The ability of the OCT parameters pBA and ONHH to predict abnormal pulsatile and static ICP is presented in Table 2. Both pBA and ONHH predicted abnormal MWA, with optimal cut-points of  $-0.65^\circ$  and  $405 \mu\text{m}$ . Their predictive ability remained significant

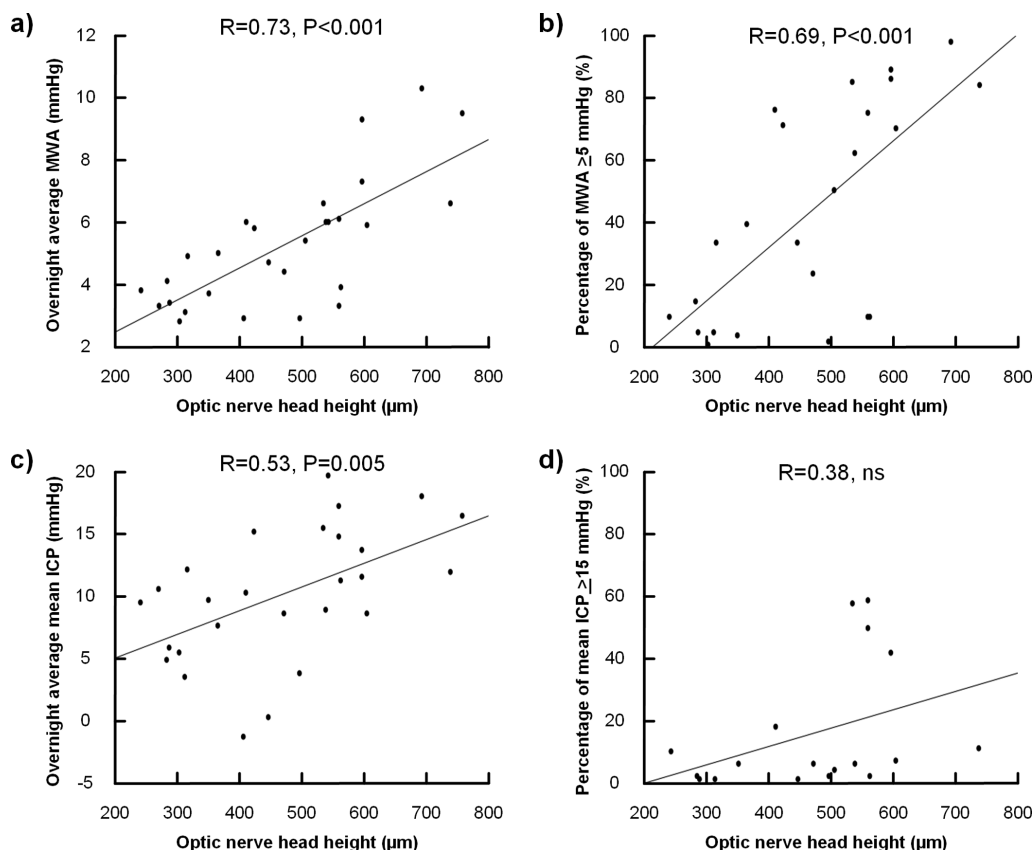


**Figure 4.** Association between the ONHH and pulsatile and static ICP scores. There was a significant positive correlation between (a) the ONHH and the average overnight MWA and (b) between the ONHH and the overnight percentage of MWA  $\geq 5$  mmHg. There also was significant positive correlation between (c) ONHH and average of overnight mean ICP but no correlation between (d) ONHH and overnight percentage mean ICP  $\geq 15$  mm Hg. Each plot shows the fit line and Pearson correlation coefficient with significance levels. ns, nonsignificant.

**Table 2.** Ability of OCT to Predict Elevated MWA and Mean ICP

OCT	ICP	Crude Estimate OR (95% CI), P Value	AUC (95% CI)	Optimal Cut-Point	Sensitivity at Cut-Point	Specificity at Cut-Point
pBA	MWA (elevated)	1.51 (1.09–2.08), 0.013	0.82 (0.66–0.98)	$-0.65^\circ$	0.75	0.92
ONHH		1.01 (1.00–1.02), 0.007	0.84 (0.70–0.99)	405 $\mu\text{m}$	0.88	0.69
pBA	Mean ICP (elevated)	1.35 (0.96–1.91), ns	0.72 (0.53–0.91)	$-0.78^\circ$	0.86	0.64
ONHH		1.01 (1.00–1.02), 0.007	0.79 (0.62–0.96)	517 $\mu\text{m}$	0.86	0.73

The predictive ability of the OCT parameters was determined by logistic regression analysis, including determination of OR and AUC with 95% confidence intervals. AUC, area under the curve; CI, confidence interval; OR, odds ratio.

after adjusting for age and BMI (Table 3). The ONHH predicted elevated mean ICP with an optimal cut-point of 517  $\mu\text{m}$  (Table 2), but this was nonsignificant after

adjusting for age and BMI (Table 3). Accordingly, both the pBA and ONHH most accurately predicted the MWA scores. Figure 5 displays the ROCs.

**Table 3.** Age and BMI-Adjusted Ability of OCT to Predict Elevated MWA and Mean ICP

OCT	ICP	Crude Estimate OR (95% CI), P Value	AUC (95% CI)
pBA	MWA (elevated)	1.98 (1.17–3.36), 0.011	0.85 (0.68–1.00)
ONHH		1.01 (1.00–1.02), 0.010	0.86 (0.72–0.99)
pBA	Mean ICP (elevated)	1.19 (0.79–1.81), ns	0.79 (0.58–0.99)
ONHH		1.01 (1.00–1.02), ns	0.84 (0.68–1.00)

The age and BMI-adjusted predictive ability of the OCT parameters was determined by logistic regression analysis, including determination of OR and the AUC with 95% confidence intervals.

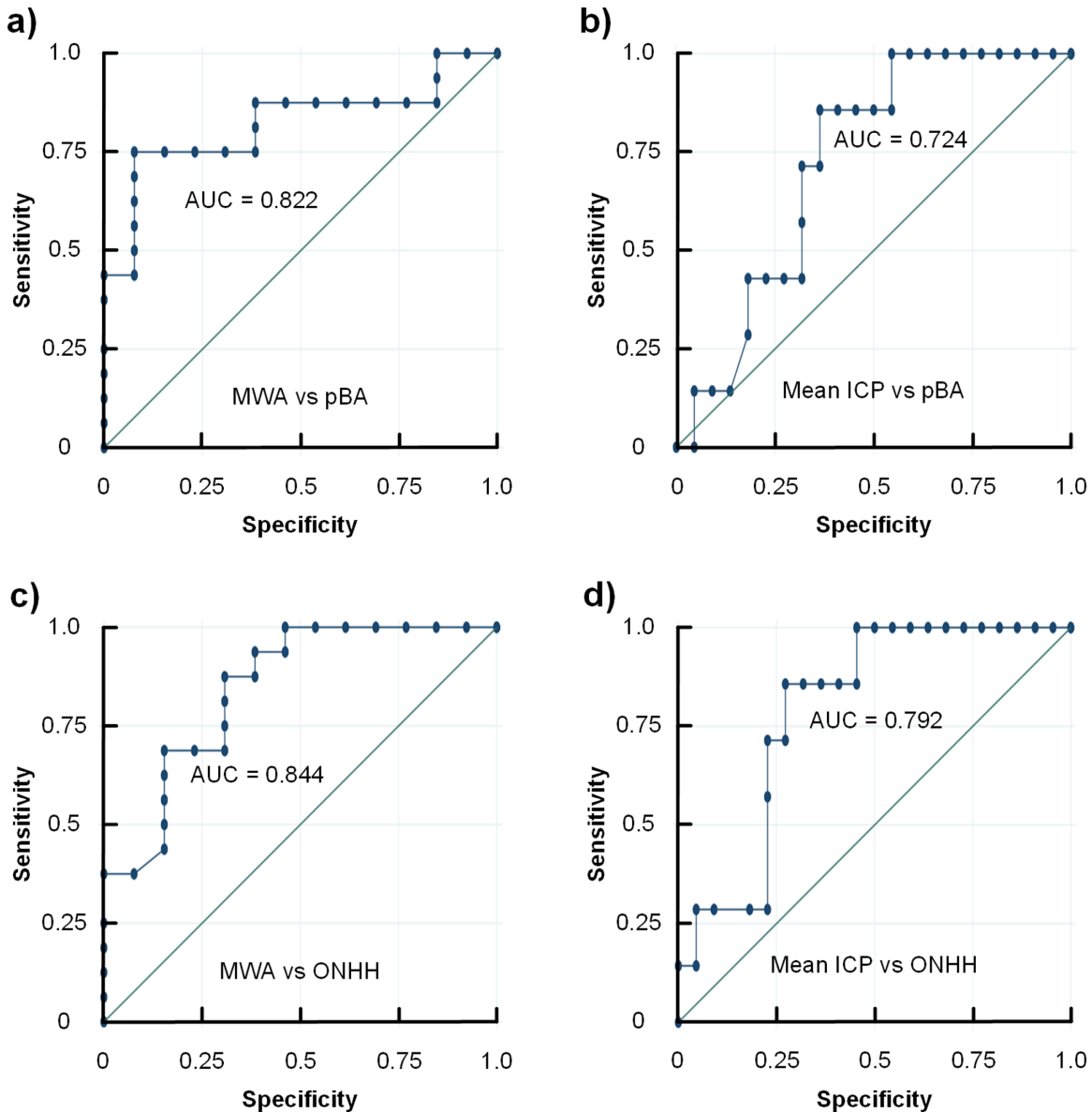


**Figure 5.** Receiver operating curves for ability of OCT parameters to predict ICP scores. The pBA showed better ability to predict (a) the overnight MWA than (b) the overnight mean ICP. Likewise, the ONHH showed better ability to predict (c) the overnight MWA than (d) the overnight mean ICP. For details about ROC results, see [Tables 2 and 3](#).

## Discussion

This study provides evidence that OCT may be used to noninvasively estimate the pulsatile ICP. The OCT parameters pBA and ONHH correlated with the overnight pulsatile ICP (MWA). The optimal cutoff values for the pBA predicted elevated MWA with a sensitivity of 75% and a specificity of 92%. Similarly, the ONHH predicted elevated MWA with a sensitivity of 88% and specificity of 69%. The OCT param-

eters could, however, not reliably predict the static ICP (mean ICP).

The present study included both a patient group with IIH diagnosed according to current criteria<sup>27</sup> and a REF group without CSF disturbances. It should be noted that patients with IIH were initially diagnosed and treated locally but referred to our hospital because of failed conservative medical treatment. Their IIH diagnosis is therefore based on observations made prior to examination in our hospital as well. Concerning the REF cohort, it is important to emphasize that

they were not healthy individuals but had various complaints and symptoms. Even though imaging and ICP measurements gave no obvious indication of CSF disturbance, we cannot conclude that this group has an entirely normal CSF function. Notably, the groups were comparable with respect to both age and BMI. As patients with IIH generally have increased BMI, it may seem peculiar that the BMI values were comparable, but we made no selection of participants based on BMI (i.e., this was incidental).

Both the pulsatile and static ICP scores were increased in the IIH group, despite prior conservative medical treatment for IIH. An abnormal MWA in the majority of the patients with IIH and mean ICP being elevated in less than half of the patients compares with previous studies in patients with IIH who had failed conservative medical treatment.<sup>28,31</sup> The MWA shows a better correlation with the intracranial compliance (i.e., intracranial pressure volume reserve capacity) than mean ICP.<sup>26</sup> Furthermore, intracranial compliance can be impaired despite normal mean ICP.<sup>32</sup> Therefore, patients with IIH may have impaired intracranial compliance even though mean ICP is within normal thresholds. Another possible reason for the abnormal pulsatile ICP may be alterations at the capillary level, which may underlie the impaired glymphatic function (i.e., impaired paravascular molecular transport) that was recently demonstrated in patients with IIH.<sup>33</sup>

The ICP scores were derived from continuous overnight measurements. Previous studies have explored various types of continuous noninvasive source signals to estimate ICP.<sup>4-7</sup> Continuous monitoring of the optic nerve with OCT is, to our knowledge, not available. Yet, a single time point examination may be used to estimate the presence of normal or abnormal ICP. Thus, OCT could serve as a method to differentiate elevated from nonelevated pulsatile ICP. A definite diagnosis of abnormal pulsatile and static ICP still requires an invasive procedure.

The pBA was significantly smaller in the IIH group than in the REF group. A smaller angle implies a more anterior position of the peripapillary Bruch's membrane. The position of this anatomic area reflects the balance between the pressure in the perioptic subarachnoid space and the intraocular pressure.<sup>34</sup> Elevated ICP relative to the intraocular pressure causes an anterior deflection. Lowering ICP has been shown to reverse the anterior deflection.<sup>19,34,35</sup> Illustrating the highly dynamic properties of this parameter, one study observed reversing of the position of the peripapillary Bruch's membrane within 1 hour after lowering the ICP.<sup>20</sup> Previous studies have also shown anterior deflection of the Bruch's membrane in patients with elevated lumbar CSF opening pressure.<sup>19,21,34,36</sup>

However, contradictory to previous findings,<sup>20,22,37</sup> we did not find any correlation between the anterior deflection and the mean ICP. There are several potential reasons for this discrepancy. Both the lumbar CSF opening pressure and the mean ICP refer to the static ICP component; these pressures are not identical, as has been previously shown by simultaneous measurements.<sup>23</sup> Moreover, a lumbar CSF pressure is measured over a very short period and may be extensively affected by stress or body position. The ICP scores presented in this study, however, were retrieved from multihour overnight measurements. The patients were resting in their beds and allowed to sleep.

Our observation of a significant correlation between pBA and MWA indicates that the abnormal pulsatile pressure fluctuations during the cardiac beat are more susceptible to cause anterior deviation of the peripapillary Bruch's membrane than a static pressure gradient. Accordingly, repetitive small cardiac-related pressure fluctuations (in the IIH group, the average overnight MWA was  $6.7 \pm 2.0$  mm Hg) seem to exert a different effect on the soft tissue than a static difference in pressure (the overnight mean ICP in IIH patients was  $13.4 \pm 5.6$  mm Hg).

We did not find between-group differences in the RNFL. An automatic algorithm for measuring the RNFL thickness is available in all OCT devices and widely used in the diagnosis and management of papilledema.<sup>13,14,38</sup> Elevated ICP compresses the optic nerve and leads to axoplasmic stasis and swelling of the retinal nerve fibers.<sup>12</sup> However, since dead axons do not swell, a major drawback of measuring the RNFL is the potentially false impression of a normal or even thin RNFL in patients with increased ICP, if optic nerve atrophy has developed. Notably, the pBA is not affected by optic atrophy. Accordingly, it may be a more reliable biomarker for noninvasive ICP estimation if atrophy has developed. Intriguing in this regard is a previous case report.<sup>19</sup> This report suggested the anterior deflection of the peripapillary Bruch's membrane to better indicate elevated ICP than the RNFL per se in a patient with optic nerve atrophy treated with CSF diversion (shunt) surgery.

The ONHH was higher in the IIH than in the REF group. Elevated ONHH has been shown to correlate with the optic nerve head volume and likely reflects the swelling and protrusion of the optic nerve head caused by the increased ICP.<sup>14</sup> The increased ONHH in the IIH group may thus reflect papilledema, although this would expectedly be accompanied by increased RNFL thickness.<sup>14,39</sup> We observed papilledema in only 7 of 20 patients with IIH, yet elevated MWA levels were seen in all but one patient with IIH. The IIH group consisted of patients who had initiated conservative



medical therapy prior to referral to the Department of Neurosurgery. Most likely, the initial therapy had alleviated the papilledema in some, resulting in thinner RNFL and a fundoscopically normal appearance of the optic disc. As the ONHH was higher in the IHH group, it may be speculated that the ONHH better reflects changes in the optic nerve head induced by elevated MWA than the RNFL.

Previous studies of the association between ONHH and ICP provide conflicting results. Two studies<sup>17,18</sup> demonstrated a correlation between the height of the optic nerve head and invasively measured mean ICP. Similarly, a third study found a trend toward a decrease in ONHH after lowering the CSF opening pressure.<sup>40</sup> Other studies, however, found no<sup>14</sup> or even a negative<sup>41</sup> association between the ONHH and the lumbar CSF opening pressure.

Some limitations of this study should be noted. First, due to the lack of an automatic algorithm in the NIDEK software for pBA and ONHH determination, these may be examiner dependent. To mitigate this potential bias, a consensus between two examiners was made. Second, for logistic reasons, we were not able to perform ICP and OCT measurements simultaneously. There was a time lag of weeks to months between the two examinations. However, except for a spinal tap in one patient and a dose increase of acetazolamide in another, no interventions were undertaken between the OCT and ICP measurements. Both examinations were performed prior to shunt implantation. Elevated MWA serves as an indication for shunt surgery and is expected to remain at abnormal levels without intervention. Thus, we are confident that the MWA was elevated at the time of OCT examination.

## Conclusions

The pBA and ONHH correlated with the pulsatile ICP and differentiated between elevated and non-elevated ICP levels. Moreover, the pBA and ONHH significantly predicted the MWA scores. Accordingly, the present method shows promise as a noninvasive way of detecting abnormal pulsatile ICP.

## Acknowledgments

The authors thank the nurse staff at the Hydrocephalus Outpatient Clinic, Department of Neurosurgery, Oslo University Hospital–Rikshospitalet and clinical research nurse, Carol Sumague, at the Depart-

ment of Ophthalmology, Oslo University Hospital–Ullevål.

Supported by the South-Eastern Norway Regional Health Authority (reference 2018020), the Norwegian Association of the Blind and Partially Sighted, and the Norwegian Glaucoma Research Foundation. The sponsor or funding organizations had no role in the design or conduct of this research.

Disclosure: **H.H. Jacobsen**, None; **Ø.K. Jørstad**, None; **M.C. Moe**, None; **G. Petrovski**, None; **A.H. Pripp**, None; **T. Sandell**, None; **P.K. Eide**, None

## References

1. Evensen KB, Eide PK. Measuring intracranial pressure by invasive, less invasive or non-invasive means: limitations and avenues for improvement. *Fluids Barriers CNS*. 2020;17:34.
2. Koskinen LO, Grayson D, Olivecrona M. The complications and the position of the Codman MicroSensor ICP device: an analysis of 549 patients and 650 Sensors. *Acta Neurochir (Wien)*. 2013;155:2141–2148, discussion 2148.
3. Binz DD, Toussaint LG, Friedman JA. Hemorrhagic complications of ventriculostomy placement: a meta-analysis. *Neurocrit Care*. 2009;10:253.
4. Evensen KB, O'Rourke M, Prieur F, Holm S, Eide PK. Non-invasive estimation of the intracranial pressure waveform from the central arterial blood pressure waveform in idiopathic normal pressure hydrocephalus patients. *Sci Rep*. 2018;8:4714.
5. Evensen KB, Paulat K, Prieur F, Holm S, Eide PK. Utility of the tympanic membrane pressure waveform for non-invasive estimation of the intracranial pressure waveform. *Sci Rep*. 2018;8:15776.
6. Ringstad G, Lindstrøm EK, Vatnehol SAS, Mardal K-A, Emblem KE, Eide PK. Non-invasive assessment of pulsatile intracranial pressure with phase-contrast magnetic resonance imaging. *PLoS One*. 2017;12:e0188896.
7. Levinsky A, Papyan S, Weinberg G, Stadheim T, Eide PK. Non-invasive estimation of static and pulsatile intracranial pressure from transcranial acoustic signals. *Med Eng Phys*. 2016;38:477–484.
8. Koskinen L-OD, Malm J, Zakelis R, Bartusis L, Ragauskas A, Eklund A. Can intracranial pressure be measured non-invasively bedside using a two-depth Doppler-technique? *J Clin Monitor Comput*. 2017;31:459–467.

9. Kimberly HH, Shah S, Marill K, Noble V. Correlation of optic nerve sheath diameter with direct measurement of intracranial pressure. *Acad Emerg Med.* 2008;15:201–204.
10. Andersen MS, Pedersen CB, Poulsen FR. A new novel method for assessing intracranial pressure using non-invasive fundus images: a pilot study. *Sci Rep.* 2020;10:13062.
11. Koziarz A, Sne N, Kegel F, et al. Bedside optic nerve ultrasonography for diagnosing increased intracranial pressure: a systematic review and meta-analysis. *Ann Intern Med.* 2019;171(12):896–905.
12. Hayreh SS. Pathogenesis of optic disc edema in raised intracranial pressure. *Prog Retin Eye Res.* 2016;50:108–144.
13. Malhotra K, Padungkiatsagul T, Moss HE. Optical coherence tomography use in idiopathic intracranial hypertension. *Ann Eye Sci.* 2020; 5:7.
14. Group OCTS-SCfNIIHS, Auinger P, Durbin M, et al. Baseline OCT measurements in the idiopathic intracranial hypertension treatment trial, part II: correlations and relationship to clinical features. *Invest Ophthalmol Vis Sci.* 2014;55:8173–8179.
15. Skau M, Yri H, Sander B, Gerds TA, Milea D, Jensen R, et al. Diagnostic value of optical coherence tomography for intracranial pressure in idiopathic intracranial hypertension. *Graefes Arch Clin Exp Ophthalmol.* 2013;251:567–574.
16. Huang D, Swanson EA, Lin CP, et al. Optical coherence tomography. *Science.* 1991;254:1178–1181.
17. Vijay V, Mollan SP, Mitchell JL, et al. Using optical coherence tomography as a surrogate of measurements of intracranial pressure in idiopathic intracranial hypertension. *JAMA Ophthalmol.* 2020;138(12):1264–1271.
18. Swanson JW, Aleman TS, Xu W, et al. Evaluation of optical coherence tomography to detect elevated intracranial pressure in children. *JAMA Ophthalmol.* 2017;135:320–328.
19. Sibony P, Kupersmith MJ, Honkanen R, Rohlf FJ, Torab-Parhiz A. Effects of lowering cerebrospinal fluid pressure on the shape of the peripapillary retina in intracranial hypertension. *Invest Ophthalmol Vis Sci.* 2014;55:8223–8231.
20. Gampa A, Vangipuram G, Shirazi Z, Moss HE. Quantitative association between peripapillary Bruch's membrane shape and intracranial pressure. *Invest Ophthalmol Vis Sci.* 2017;58:2739–2745.
21. Sibony P, Kupersmith MJ, Rohlf FJ. Shape analysis of the peripapillary RPE layer in papilledema and ischemic optic neuropathy. *Invest Ophthalmol Vis Sci.* 2011;52:7987–7995.
22. Patel MD, Malhotra K, Shirazi Z, Moss HE. Methods for quantifying optic disc volume and peripapillary deflection volume using radial optical coherence tomography scans and association with intracranial pressure. *Front Neurol.* 2019;10:798.
23. Eide PK, Brean A. Lumbar cerebrospinal fluid pressure waves versus intracranial pressure waves in idiopathic normal pressure hydrocephalus. *Br J Neurosurg.* 2006;20:407–414.
24. Czosnyka M, Pickard JD. Monitoring and interpretation of intracranial pressure. *J Neurol Neurosurg Psychiatry.* 2004;75:813–821.
25. Eide PK. A new method for processing of continuous intracranial pressure signals. *Med Eng Phys.* 2006;28:579–587.
26. Eide PK. The correlation between pulsatile intracranial pressure and indices of intracranial pressure-volume reserve capacity: results from ventricular infusion testing. *J Neurosurg.* 2016;125:1493–1503.
27. Mollan SP, Davies B, Silver NC, et al. Idiopathic intracranial hypertension: consensus guidelines on management. *J Neurol Neurosurg Psychiatry.* 2018;89:1088–1100.
28. Eide PK, Kerty E. Static and pulsatile intracranial pressure in idiopathic intracranial hypertension. *Clin Neurol Neurosurg.* 2011;113:123–128.
29. Eide PK, Sorteberg W. Diagnostic intracranial pressure monitoring and surgical management in idiopathic normal pressure hydrocephalus: a 6-year review of 214 patients. *Neurosurgery.* 2010;66:80–91.
30. Clayton P. CUTPT: Stata module for empirical estimation of cutpoint for a diagnostic test. *Statistical Software Components.* 2013. <https://EconPapers.repec.org/RePEc:boc:bocode:s457719>
31. Eide PK. Abnormal intracranial pulse pressure amplitude despite normalized static intracranial pressure in idiopathic intracranial hypertension refractory to conservative medical therapy. *Life (Basel).* 2021;11(6):537.
32. Eide PK, Sorteberg W. Association among intracranial compliance, intracranial pulse pressure amplitude and intracranial pressure in patients with intracranial bleeds. *Neurol Res.* 2007;29:798–802.
33. Eide PK, Pripp AH, Ringstad G, Valnes LM. Impaired glymphatic function in idiopathic intracranial hypertension. *Brain Commun.* 2021;3:fcab043.
34. Kupersmith MJ, Sibony P, Mandel G, Durbin M, Kardon RH. Optical coherence tomography

- of the swollen optic nerve head: deformation of the peripapillary retinal pigment epithelium layer in papilledema. *Invest Ophthalmol Vis Sci.* 2011;52:6558–6564.
35. Wang J-K, Kardon RH, Ledolter J, et al. Peripapillary retinal pigment epithelium layer shape changes from acetazolamide treatment in the idiopathic intracranial hypertension treatment trial. *Invest Ophthalmol Vis Sci.* 2017;58:2554–2565.
  36. Sibony PA, Kupersmith MJ. Geometric morphometrics of the peripapillary RPE layer by OCT. *Invest Ophthalmol Vis Sci.* 2011;52:3004.
  37. Malhotra K, Patel MD, Shirazi Z, Moss HE. Association between peripapillary Bruch's membrane shape and intracranial pressure: effect of image acquisition pattern and image analysis method, a preliminary study. *Front Neurol.* 2018;9:1137.
  38. Ophir A, Karatas M, Ramirez JA, Inzelberg R. OCT and chronic papilledema. *Ophthalmology.* 2005;112:2238.
  39. Karam EZ, Hedges TR. Optical coherence tomography of the retinal nerve fibre layer in mild papilloedema and pseudopapilloedema. *Br J Ophthalmol.* 2005;89:294–298.
  40. Anand A, Pass A, Urfy MZ, et al. Optical coherence tomography of the optic nerve head detects acute changes in intracranial pressure. *J Clin Neurosci.* 2016;29:73–76.
  41. Kaufhold F, Kadas EM, Schmidt C, et al. Optic nerve head quantification in idiopathic intracranial hypertension by spectral domain OCT. *PLoS One.* 2012;7:e36965.